

[REDACTED]

NACA

249  
Copy  
RM L54A21

TECH LIBRARY KAFB, NM

0144321

# RESEARCH MEMORANDUM

WIND-TUNNEL INVESTIGATION AT HIGH SUBSONIC SPEEDS OF THE  
EFFECTS OF WING-MOUNTED EXTERNAL STORES ON THE  
LOADING AND AERODYNAMIC CHARACTERISTICS  
IN PITCH OF A 45° SWEPTBACK WING  
COMBINED WITH A FUSELAGE

By H. Norman Silvers, Thomas J. King, Jr.,  
and William J. Alford, Jr.

Langley Aeronautical Laboratory  
Langley Field, Va.

[REDACTED]  
[REDACTED]  
[REDACTED]  
**NATIONAL ADVISORY COMMITTEE  
FOR AERONAUTICS**

WASHINGTON

March 23, 1954

[REDACTED]

342

Classification canceled or changed to UNCLASSIFIED

By Authority of NASA Tech Prod Admin Comptt #124  
(OFFICER AUTHORIZED TO CHANGE)

By ..... 10 FEB 58  
NAME AND

GRADE OF OFFICER MAKING CHANGE)

28 Mat 61  
DATE



0144321

1G

NACA RM L54A21

~~CONFIDENTIAL~~

## NATIONAL ADVISORY COMMITTEE FOR AERONAUTICS

## RESEARCH MEMORANDUM

WIND-TUNNEL INVESTIGATION AT HIGH SUBSONIC SPEEDS OF THE  
EFFECTS OF WING-MOUNTED EXTERNAL STORES ON THE  
LOADING AND AERODYNAMIC CHARACTERISTICSIN PITCH OF A 45° SWEPTBACK WING  
COMBINED WITH A FUSELAGEBy H. Norman Silvers, Thomas J. King, Jr.,  
and William J. Alford, Jr.

## SUMMARY

An investigation has been made of the effect of wing-mounted external stores on the loading and the aerodynamic characteristics in pitch of a 45° sweptback wing combined with a fuselage in a Mach number range from 0.50 to 0.91. The store arrangements investigated consisted of stores mounted at the wing tips, stores mounted inboard on the wing undersurface at 46-percent semispan, and stores in both the tip and the inboard locations. The stores had an ogive-cylinder shape and a fineness ratio of 9.34.

The results of the investigation indicate that the tip-mounted stores increased the loading at the wing tips at low angles of attack, whereas the inboard stores increased the tip loading and decreased the inboard loading at the higher angles of attack and lower Mach numbers. The loading changes associated with the tip stores resulted in an increase in lift-curve slope and a rearward movement in the aerodynamic-center location of the complete model; while the inboard stores acted much like fences and chord-extensions in that they extended the lift-coefficient range prior to the onset of a type of longitudinal instability known as pitch-up. The combined arrangement of stores (inboard and tip) showed characteristics which represented a combination of those of the individual components of this arrangement.

~~CONFIDENTIAL~~*Han 11-392*

## INTRODUCTION

The National Advisory Committee for Aeronautics is conducting investigations of nacelles and external stores for use on high-speed aircraft. These investigations are primarily concerned with the effects of stores on the performance characteristics of wing-fuselage combinations. In addition to the performance studies, investigations are being made of the aerodynamic loading characteristics of wings with stores and the loadings on stores in the presence of wings. In reference 1 available data on the aerodynamic loads associated with external-store installations are reviewed briefly. This paper presents results obtained on the effect of several arrangements of external stores on the aerodynamic loading characteristics in pitch obtained from pressure measurements on a 45° sweptback wing combined with a fuselage and also indicates briefly the effects of the store arrangements on the force and moment characteristics of the wing-fuselage model. Some of the data presented herein are also contained in reference 1.

## SYMBOLS

$C_L$	lift coefficient, $\frac{\text{Lift}}{qS}$
$C_D$	drag coefficient, $\frac{\text{Drag}}{qS}$
$C_m$	pitching-moment coefficient, $\frac{\text{Pitching moment}}{qS\bar{c}}$
$c_n$	section normal-force coefficient, $\frac{\text{Normal force}}{qc}$
$C_{N_e}$	exposed wing-panel normal-force coefficient, $\frac{2}{b_e} \int_0^{b_e/2} \left( c_n \frac{c}{c_{av}} \right) dy_e$
$\alpha$	angle of attack of the fuselage center line, deg
$y$	lateral distance, measured from the plane of symmetry
$y_e$	lateral distance, measured from wing-fuselage intersection

$\frac{y_{cp}}{b_e/2}$	lateral center-of-pressure position, fraction of exposed wing semispan
$x/c$	distance from wing leading edge, fraction of local chord
$x_{cp}/c$	local chordwise center-of-pressure position, fraction of local chord
P	pressure coefficient, $\frac{p_l - p}{q}$
S	wing area, 2.25 sq ft
b	wing span, 3.00 ft
$b_e/2$	exposed wing semispan, measured from wing-fuselage intersection
$\bar{c}$	mean aerodynamic chord $\frac{2}{S} \int_0^{b/2} c^2 dy$ (using theoretical tip), 0.765 ft
c	local wing chord
$c_{av}$	average wing chord, 0.75 ft
d	diameter of store, 0.167 ft
l	length of store, 1.544 ft
q	free-stream dynamic pressure, lb/sq ft
$p_l$	local static pressure
p	free-stream static pressure
M	Mach number

$$C_{I_\alpha} = \left( \frac{\partial C_L}{\partial \alpha} \right)_{M, \alpha=0^\circ}$$

$$C_m C_L = \left( \frac{\partial C_m}{\partial C_L} \right)_{M, C_L=0^\circ}$$

## Subscripts:

- e exposed wing panel from wing-fuselage intersection to the theoretical tip
- f fuselage
- b body of external store installation

## APPARATUS AND MODELS

A drawing showing the model with one arrangement of stores is presented in figure 1. The wing which had the quarter-chord line swept back  $45^{\circ}$  was of aspect ratio 4.0, taper ratio 0.6, and had NACA 65A006 airfoil sections parallel to the airstream. The wing was of composite construction, consisting of a steel core with a bismuth-tin covering to give the desired contour. The fuselage was a body of revolution having a parabolic shape defined by the ordinates presented in table I. The wing was mounted in a midwing arrangement with no incidence.

The wing of the model was equipped with pressure orifices at semi-span locations of 0.2, 0.4, 0.6, 0.8, and 0.95. The chordwise locations of the pressure orifices are presented in table II. Pressure measurements were indicated on a multitube manometer board and were recorded photographically.

Pressure measurements were obtained with the fuselage attached directly to the hollow sting support. The pressure tubes from wing orifices passed through the sting support to the exterior of the test section. The pressure tubes were removed for the force and moment measurements and the fuselage was attached to the sting support by a strain-gage balance.

The shape of the external store was generated by the revolution of a profile made of ogival nose and tail sections connected by a constant-diameter section. The fineness ratio of the store was 9.34. All stores were of the same size and shape and were mounted with no incidence as shown in figure 1. Ordinates of the store are presented in table III.

External stores were investigated in two spanwise locations (fig. 1) - an inboard and a wing-tip location. In each location two stores were located equidistant from the plane of symmetry. In addition, tests were made with a total of four stores on the wing, two in each spanwise location.

## TESTS

Tests were made in the Langley high-speed 7- by 10-foot tunnel through a Mach number range that extended from 0.50 to 0.91. The angle-of-attack range over which pressure measurements were made extended from  $0^\circ$  to about  $24^\circ$  for the model without stores and for the model with the tip-store arrangement, and from  $0^\circ$  to about  $12^\circ$  for the other store arrangements. The angle-of-attack range over which force and moment measurements were made extended from  $-2^\circ$  to about  $19^\circ$  at low Mach numbers and to about  $13^\circ$  at high Mach numbers. The angle of sideslip of the model was zero throughout this investigation.

The Reynolds number variation with Mach number, based on the mean aerodynamic chord, is presented in figure 2.

## CORRECTIONS

Blocking corrections applied to Mach number and dynamic pressure were determined by the velocity-ratio method of reference 2, which utilizes experimental pressures measured at the tunnel wall opposite the model. The correction to Mach number increased slightly with increase in speed and at  $M = 0.90$  was 0.01.

The jet-boundary corrections applied to lift and drag were calculated by the method of reference 3. The corrections to pitching moment were considered negligible. No support tares have been applied, but, as indicated in reference 4, they are believed to be small. Drag data have been corrected to correspond to a pressure at the base of the fuselage equal to free-stream static pressure. This correction, which was added to the measured drag coefficient amounted to a drag-coefficient increment that increased from a value of 0.0010 at  $M = 0.50$  to 0.0030 at  $M = 0.91$ . This correction did not vary appreciably with angle of attack. It has been indicated in reference 5 that stores do not affect this correction.

Corrections have been applied to the angles of attack of the model due to deflection of the sting support and the strain-gage balance on the basis of the loads developed during force tests. Pressure data are presented at an average angle of attack that has been corrected for deflection of the support system. No corrections have been applied to the results presented in the present paper to account for aeroelastic distortion of the wing. The effects of aeroelasticity on the force and moment results for the wing-fuselage combination have been determined and are presented in reference 6.

## DISCUSSION

## Presentation of Results

The results of this investigation are presented in the following figures:

## Figure

## Loading characteristics:

Span loading . . . . .	3 and 4
Lateral center-of-pressure locations . . . . .	5 and 6
Normalized span load distribution . . . . .	7
Section normal-force coefficient . . . . .	8 and 9
Chord loading . . . . .	10 and 11
Local chordwise center-of-pressure locations . . . . .	12 and 13

## Aerodynamic characteristics:

Aerodynamic characteristics . . . . .	14
Summary of aerodynamic characteristics . . . . .	15

## Loading Characteristics

The spanwise distribution of loading over the wing panel (fig. 3) indicates that the effects of the tip-mounted stores on the wing-loading characteristics are small except at the extreme tips of the wing. The tip stores produce an additional loading at the wing tips that is a larger fraction of the total loading at the lower angles of attack than at the higher angles. The additional wing loading produces outboard movements in the lateral centers of pressure (fig. 5) which could increase the strength requirements of inboard sections of the wing structure. This condition may be particularly important at high-speed low-altitude maneuvering attitudes.

Two methods are available for computing the wing loadings with tip stores (refs. 7 and 8). Both methods yield similar results. The method of reference 7 was used herein to compare the estimated effects of the tip store with the experimental results. In figure 7 are presented the calculated and the experimental increments in loading due to the tip store and the normalized load distributions. The calculated increments are the differences between load distributions for the wing alone and the wing with the tip store calculated using five semispan locations of the control points as suggested in reference 7. Inclusion of the fuselage effect in the calculations would have no effect on the calculated changes. The calculated load distribution presented in figure 7 for the wing alone was determined by using 10 semispan locations of the control

points (ref. 9). In order to show the load distribution of the wing with the tip store, the incremental loading obtained from the 5-control-point calculation was added to the load distribution of the 10-control-point calculation for the wing alone.

The incremental loadings indicate that the method of reference 7 predicts fairly well the effect of the tip store. The application of this method is limited to flow regimes that do not violate the assumptions of potential flow. This limits the correlation of this method with the experimental results in the present paper to Mach numbers of 0.70 and angles of attack of about  $4^{\circ}$ .

It is pointed out that the experimental pressure distributions and span-loading results include the effects of some deformation of the wing due to aeroelasticity. Estimates indicate that, for the results presented in figure 7, the effects of aeroelasticity are negligible.

The additional loading at the wing tip due to the stores results in increased section-lift-curve slopes at the tip sections (fig. 8). The section lift curves also show that the tip stores had little effect on the angle of attack at which section maximum lift was reached.

The most significant change in wing-span loadings with the inboard external stores occurs at the highest angles of attack investigated ( $\alpha = 12.5^{\circ}$  to  $12.8^{\circ}$ ), where a redistribution of loading equivalent to increased tip loading and decreased inboard loading takes place (fig. 4). The inboard store increases the angle of attack at which section maximum lift is obtained at  $0.80b/2$  (fig. 9) but decreases the angle of attack for section maximum lift at  $0.40b/2$ . This, of course, produces an outboard shift in the lateral center-of-pressure location (fig. 6) which has a tendency to alleviate the adverse stability effects associated with loss in lift at the tips of sweptback wings. This effect of the inboard store is greatly reduced at a Mach number of 0.91 (fig. 9). The inboard store thus appears to behave in much the same way as fences, chord-extensions, and other auxiliary devices designed for swept wings to extend the angle-of-attack range before loss in wing-tip loading occurs (refs. 10, 11, and 12).

The combined arrangement of inboard and tip stores shows the characteristics of each of the individual arrangements (figs. 3 and 4). At low angles of attack, the combined arrangement produces increased tip loadings that are proportional to angle of attack changes similar to those shown with the tip stores. At the higher angles of attack, this arrangement produces a redistribution of span loading similar to that obtained with the inboard store.

The effects of each arrangement of external store on the local chordwise loading of the wing are shown in figures 10 and 11 for conditions representing the largest changes in wing-span loading. The

local chordwise center-of-pressure locations (figs. 12 and 13) show that, except for what are probably localized changes with the inboard stores at  $0.40b/2$  station, there was little change in  $x_{cp}/c$  due to the tip stores or to the combined arrangement of inboard and tip stores at the lower angles of attack ( $\alpha \approx 4^\circ$ ). At a nominal angle of attack of  $12^\circ$  and  $0.60b/2$ , due to the effects of the inboard store on the loading characteristics of the wing, a forward movement in  $x_{cp}/c$  of about  $0.15c$  takes place at  $M = 0.50$ .

#### Aerodynamic Characteristics

The increase in tip loading produced by the tip stores together with the loading on the stores increases the lift-curve slopes of the complete model (fig. 15) and, because of wing sweep, results in rearward movements of the aerodynamic center. On the other hand, the inboard stores, which have little effect on the loading characteristics at the lower angles of attack, also have little effect on either the lift-curve slope or the aerodynamic-center locations. At the higher angles of attack, the changes in loading due to the inboard stores are evidenced by increases of the lift coefficients at the lower Mach numbers (fig. 14) prior to the onset of a type of longitudinal instability known as pitch-up. The increases in lift coefficients at which instabilities occur, obtained with this arrangement of stores, are as large as those obtained with fences, chord-extensions, or other devices specifically designed to promote wing-tip loading at the higher angles of attack.

The drag characteristics (fig. 15) of the model without and with the several store arrangements were obtained from tests run at zero lift coefficient through the Mach number range. These results show that the drag with the tip stores is substantially lower than the drag with the inboard stores. Since the viscous drag is essentially the same for both installations, the lower drag of the tip installation is probably due to lower interference. The drag of the installation with both the inboard and the tip stores is about the same as the sum of the incremental drags of the individual components of this installation.

#### CONCLUSIONS

An investigation of the effects of wing-mounted external stores in the Mach number range from 0.50 to 0.91 on the loading and the aerodynamic characteristics in pitch of a  $45^\circ$  sweptback wing combined with a fuselage indicate the following conclusions:

1. The tip-mounted store produced an increase in loading at the wing tip that was proportional to the angle of attack at the lower angles, which

together with the loading on the store resulted in an increase in lift-curve slopes of the complete model and a rearward movement of the aerodynamic-center locations.

2. The inboard store produced a redistribution of wing loading at the higher angles of attack and at Mach numbers less than about 0.91 and was equivalent to an increase in tip loading and a loss in inboard loading. This effect was much like the effects produced by fences and chord-extensions in that it resulted in an extension to the lift-coefficient range prior to the onset of a type of longitudinal instability known as pitch-up.

3. The combined arrangement of inboard and tip stores produced changes in loading that represented a combination of those of the individual components of this arrangement.

Langley Aeronautical Laboratory,  
National Advisory Committee for Aeronautics,  
Langley Field, Va., January 7, 1954.

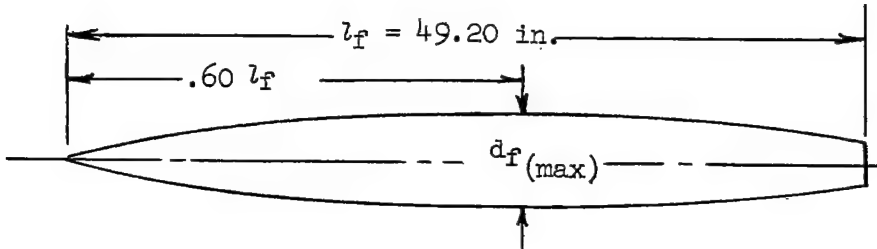
## REFERENCES

1. Silvers, H. Norman, and O'Bryan, Thomas C.: Some Notes on the Aerodynamic Loads Associated With External-Store Installations. NACA RM L53E06a, 1953.
2. Hensel, Rudolph W.: Rectangular-Wind-Tunnel Blocking Corrections Using the Velocity-Ratio Method. NACA TN 2372, 1951.
3. Gillis, Clarence L., Polhamus, Edward C., and Gray, Joseph L., Jr.: Charts for Determining Jet-Boundary Corrections for Complete Models in 7- by 10-Foot Closed Rectangular Wind Tunnels. NACA WR L-123, 1945. (Formerly NACA ARR L5G31.)
4. Osborne, Robert S.: High-Speed Wind-Tunnel Investigation of the Longitudinal Stability and Control Characteristics of a 1/16-Scale Model of the D-558-2 Research Airplane at High Subsonic Mach Numbers and at a Mach Number of 1.2. NACA RM L9C04, 1949.
5. Silvers, H. Norman, and King, Thomas J., Jr.: Investigation at High Subsonic Speeds of Bodies Mounted From the Wing of an Unswept-Wing-Fuselage Model, Including Measurements of Body Loads. NACA RM L52J08, 1952.
6. Kuhn, Richard E., and Wiggins, James W.: Wind-Tunnel Investigation of the Aerodynamic Characteristics in Pitch of Wing-Fuselage Combinations at High Subsonic Speeds. Aspect-Ratio Series. NACA RM L52A29, 1952.
7. Robinson, Samuel W., Jr., and Zlotnick, Martin: A Method for Calculating the Aerodynamic Loading on Wing--Tip-Tank Combinations in Subsonic Flow. NACA RM L53B18, 1953.
8. Hartley, D. E.: Theoretical Load Distributions on Wings With Tip-Tanks. Rep. No. Aero. 2469, British R.A.E., June, 1952.
9. Campbell, George S.: A Finite-Step Method for the Calculation of Span Loadings of Unusual Plan Forms. NACA RM L50L13, 1951.
10. Goodson, Kenneth W., and Few, Albert G., Jr.: Effect of Leading-Edge Chord-Extensions on Subsonic and Transonic Aerodynamic Characteristics of Three Models Having 45° Sweptback Wings of Aspect Ratio 4. NACA RM L52K21, 1953.

11. Spreeman, Kenneth P., and Alford, William J., Jr.: Investigation of the Effects of Leading-Edge Chord-Extensions and Fences in Combination With Leading-Edge Flaps on the Aerodynamic Characteristics at Mach Numbers From 0.40 to 0.93 of a  $45^{\circ}$  Sweptback Wing of Aspect Ratio 4. NACA RM L53A09a, 1953.
12. Wiggins, James W., and Kuhn, Richard E.: Wind-Tunnel Investigation of the Effects of Steady Rolling on the Aerodynamic Loading Characteristics of a  $45^{\circ}$  Sweptback Wing at High Subsonic Speeds. NACA RM L53J01a, 1953.

TABLE I.- FUSELAGE ORDINATES

[Basic fineness ratio 12, actual fineness ratio 10 achieved by cutting off rear portion of body]



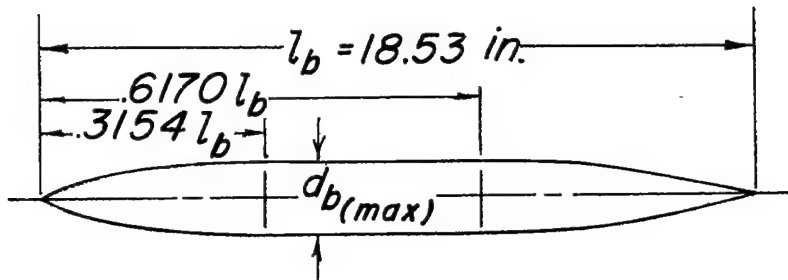
ordinates, percent length	
station	radius
0	0
.60	.28
.90	.36
1.50	.51
3.00	.87
6.00	1.45
9.00	1.94
12.00	2.37
18.00	3.11
24.00	3.71
30.00	4.16
36.00	4.49
42.00	4.72
48.00	4.88
54.00	4.97
60.00	5.00
66.00	4.96
72.00	4.83
78.00	4.61
84.00	4.28
90.00	3.75
96.00	3.03
100.00	2.50
L.E. radius = $0.0006 l_f$	

TABLE II.- CHORDWISE LOCATION OF PRESSURE ORIFICES, x/c

$\frac{y}{b/2} = 0.20$		$\frac{y}{b/2} = 0.40$		$\frac{y}{b/2} = 0.60$		$\frac{y}{b/2} = 0.80$		$\frac{y}{b/2} = 0.95$	
Upper	Lower								
0	0	0	0	0	0	0	0	0	0
.025	.025	.025	.025	.025	.025	.025	.025	.025	.025
.075	.075	.075	.075	.075	.075	.075	.075	.075	.075
.15	.15	.15	.15	.15	.15	.15	-----	.15	.15
.25	.25	.25	.25	-----	.25	.25	.25	.25	.25
.35	.35	.35	.35	.35	.35	.35	-----	.35	.35
.45	.45	.45	.45	.45	.45	.45	.45	.45	.45
.55	.55	.55	.55	.55	.55	.55	.55	.55	.55
.65	.65	.65	.65	-----	.65	-----	-----	.65	.65
-----	.75	.75	.75	.75	.75	.75	.75	.75	.75
.85	.85	.85	.85	.85	.85	.85	-----	.85	.85
.95	-----	.95	.95	.95	.95	.95	.95	.95	.95
-----	-----	1.00	1.00	-----	-----	-----	-----	-----	-----

TABLE III.- STORE ORDINATES

[Fineness ratio 9.34]



Ordinates, percent length	
Station	Radius
0	0
.36	.30
1.21	.73
3.04	1.44
4.87	2.09
6.71	2.65
8.26	3.07
9.15	3.29
9.69	3.44
10.84	3.70
11.99	3.94
13.14	4.12
14.29	4.30
15.44	4.44
17.74	4.70
20.04	4.92
22.34	5.08
24.64	5.20
26.94	5.30
29.24	5.34
31.54	5.36
61.70	5.36
68.69	5.20
74.95	4.76
81.22	3.94
87.48	2.76
90.60	2.11
93.75	1.42
96.89	.72
98.44	.36
100.00	0

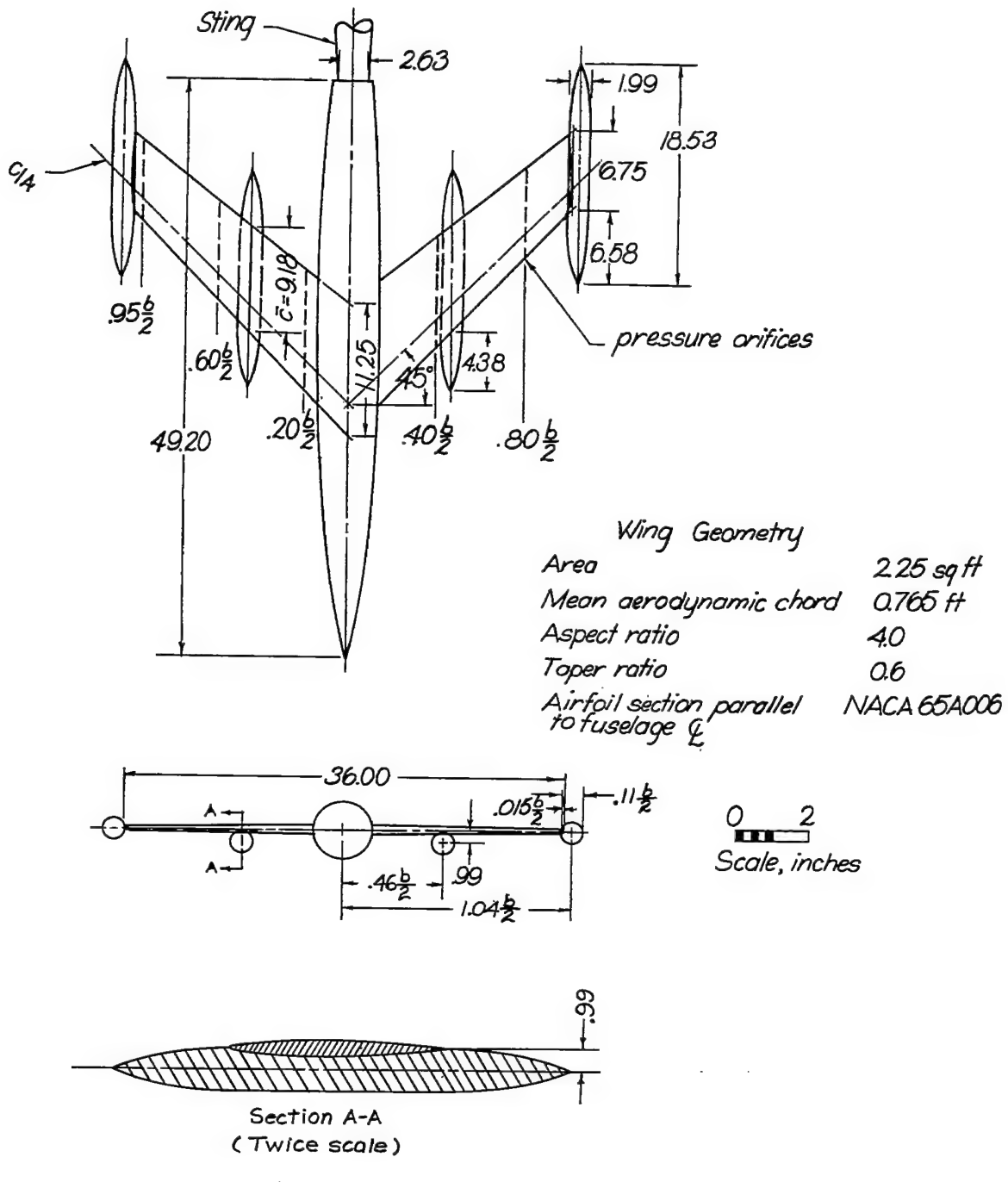


Figure 1.- A drawing of the test model showing one arrangement of the external stores investigated.

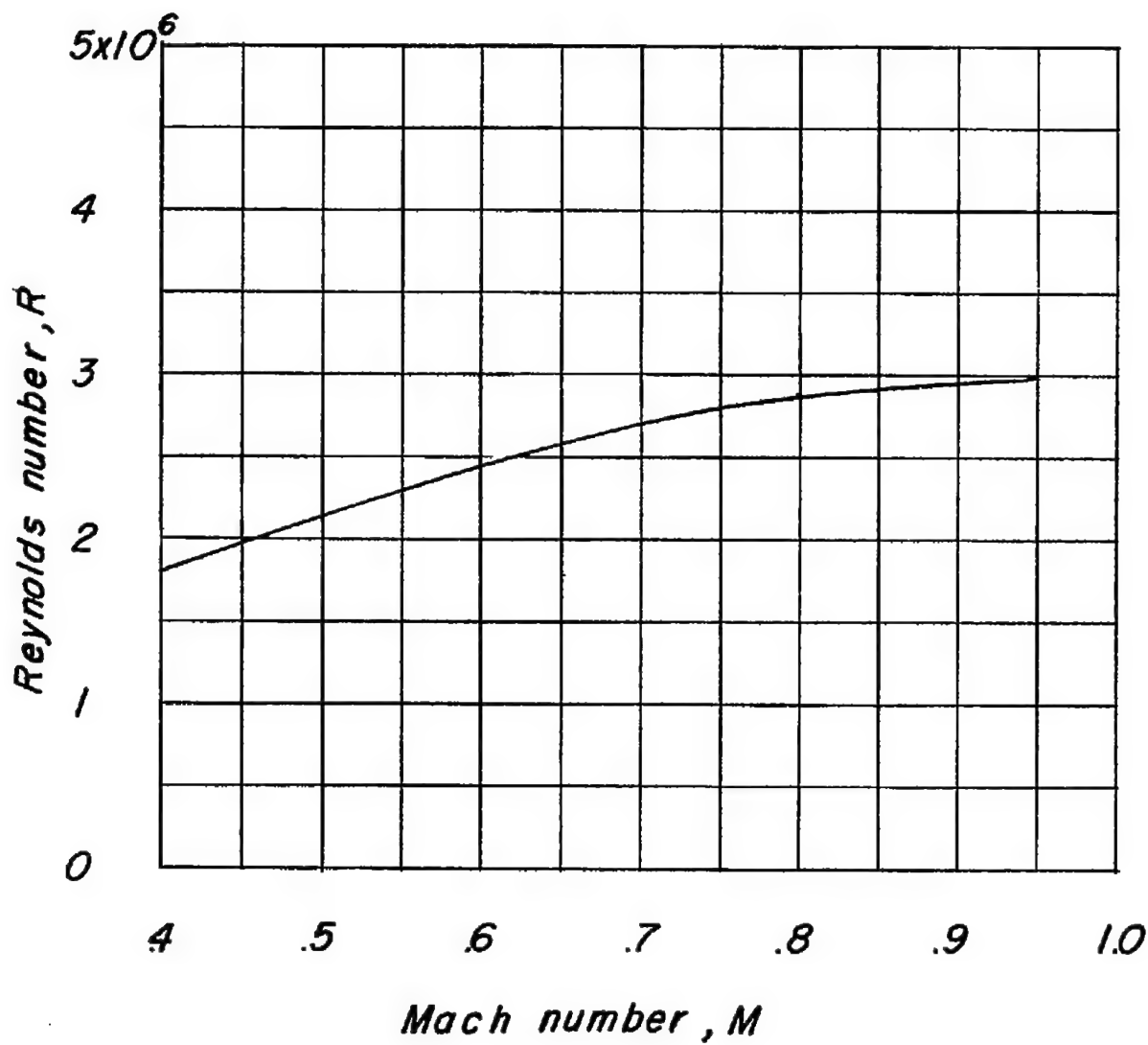


Figure 2.- Variation of Reynolds number with Mach number for the model.

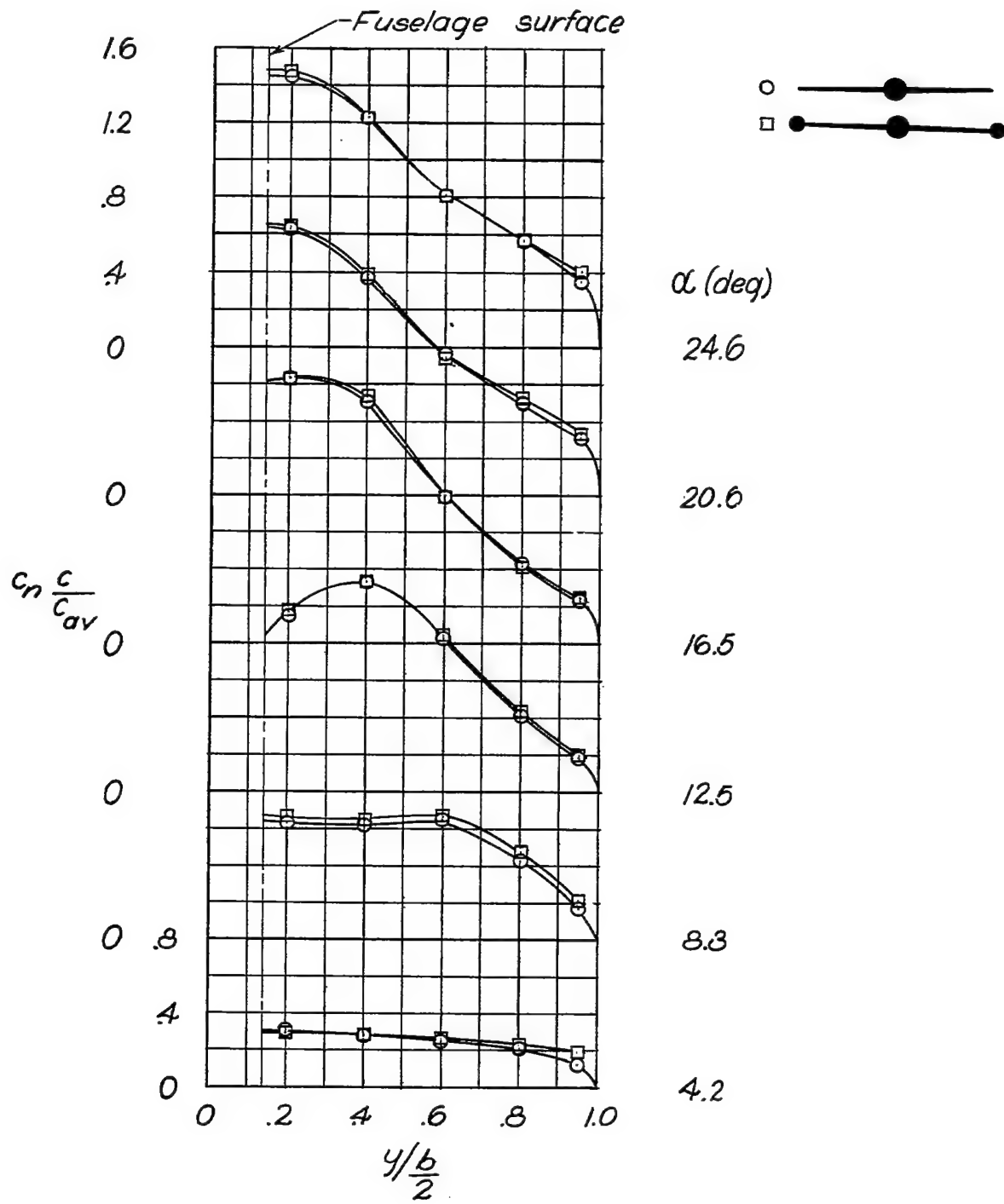
(a)  $M = 0.50$ .

Figure 3.- Span loading of the model without external stores and with the tip external stores.

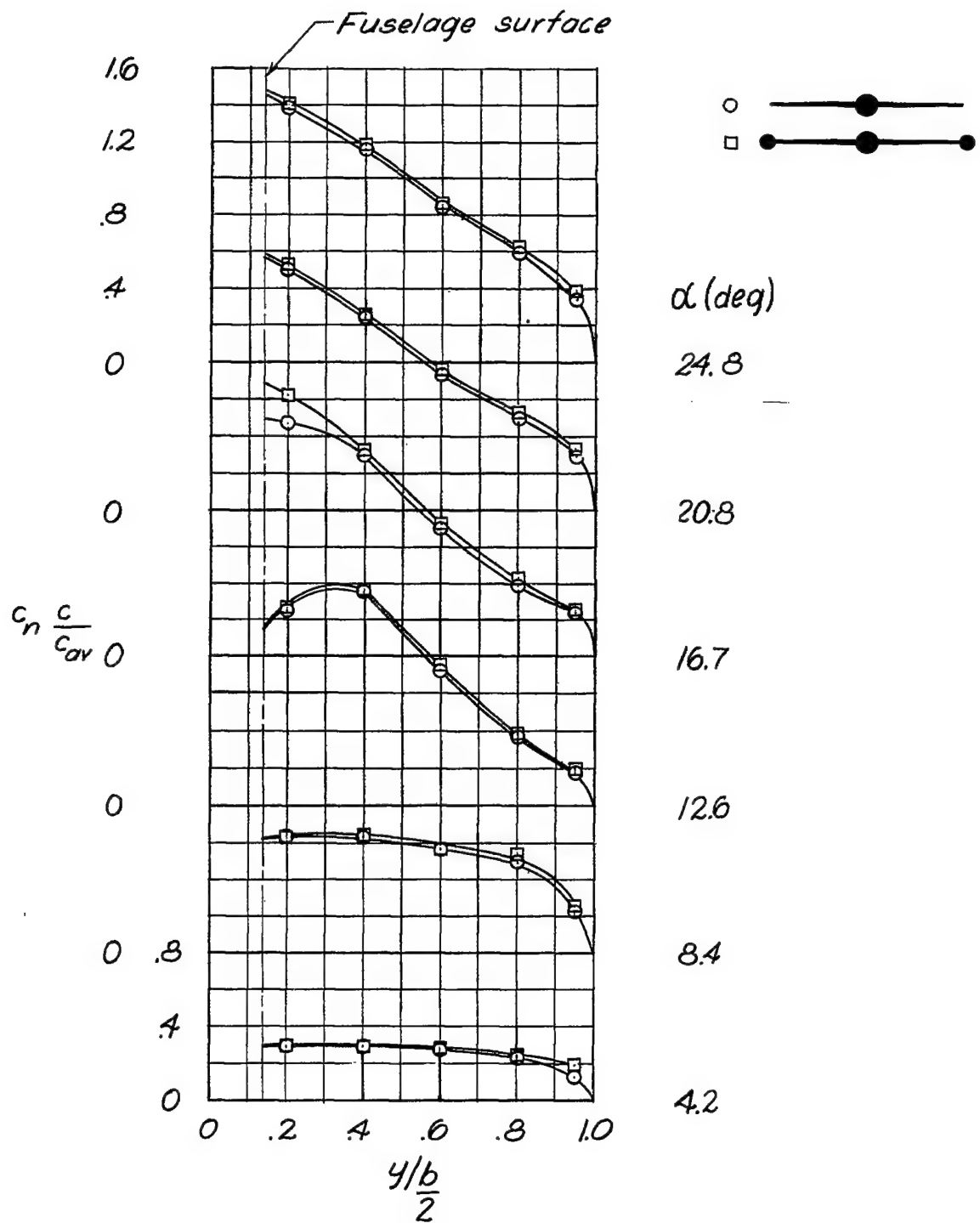
(b)  $M = 0.70.$ 

Figure 3.- Continued.

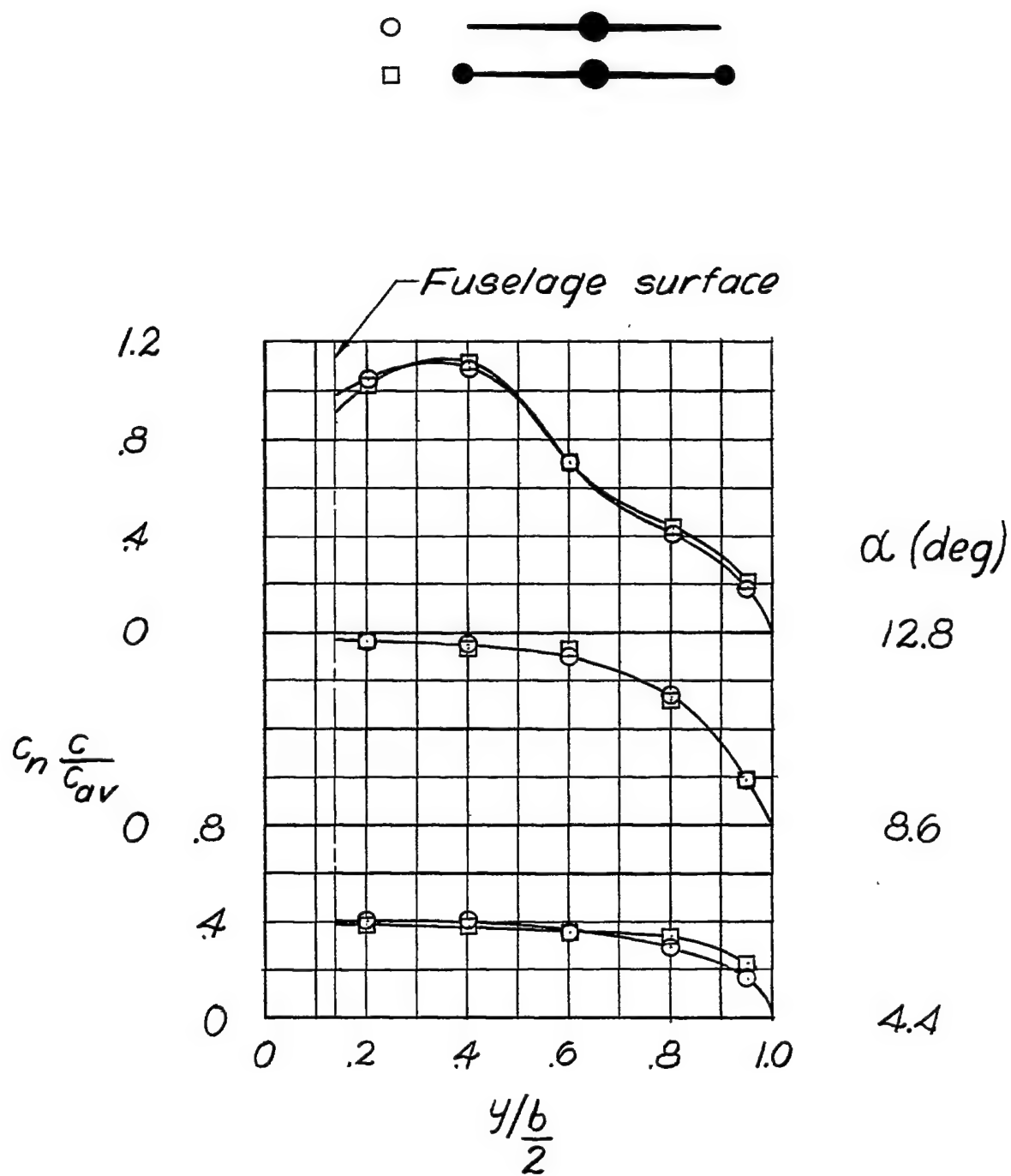
(c)  $M = 0.91.$ 

Figure 3.- Concluded.

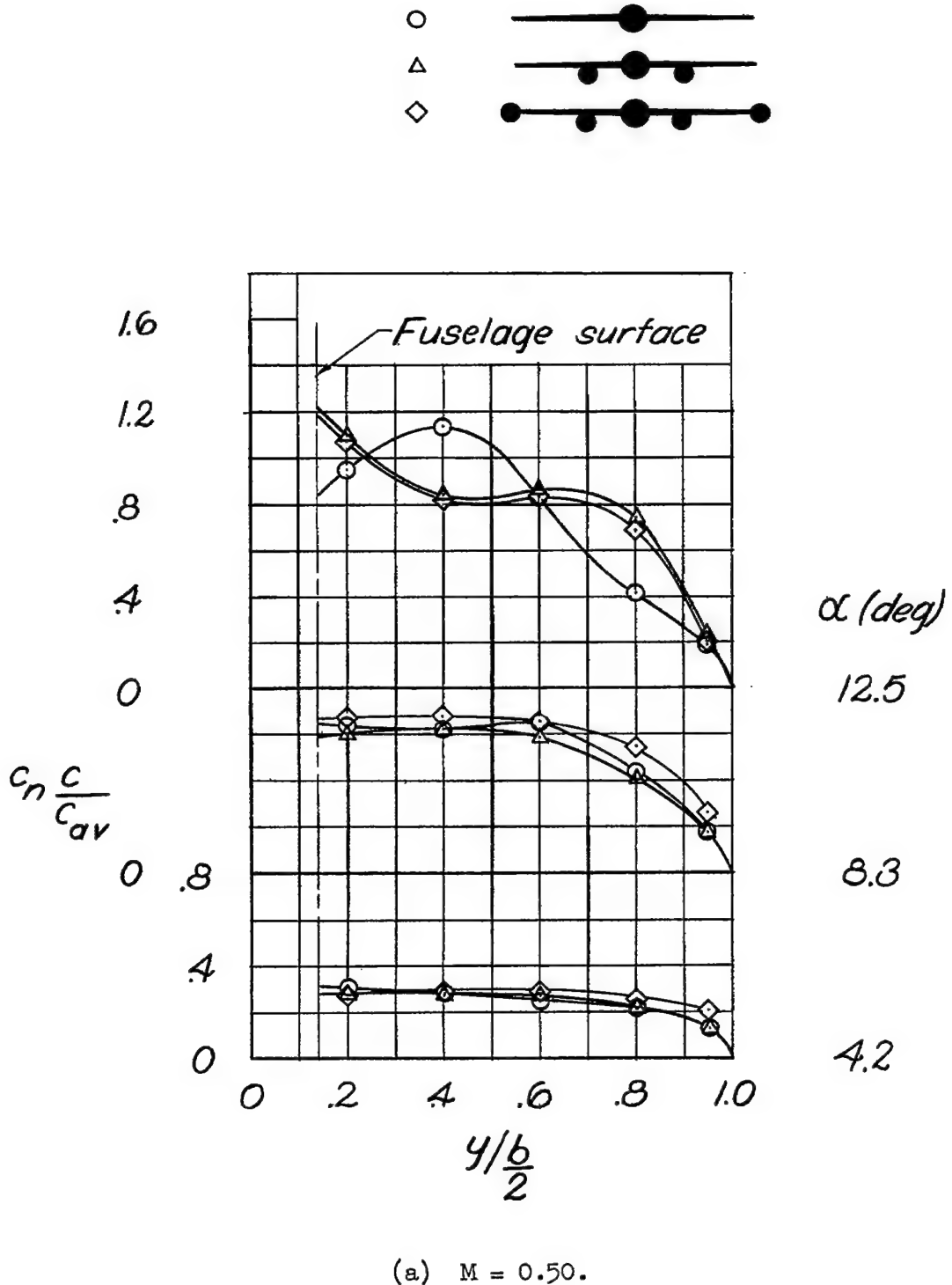


Figure 4.- Span loading of the model without external stores, with the inboard external stores, and with the inboard and tip external stores in combination.

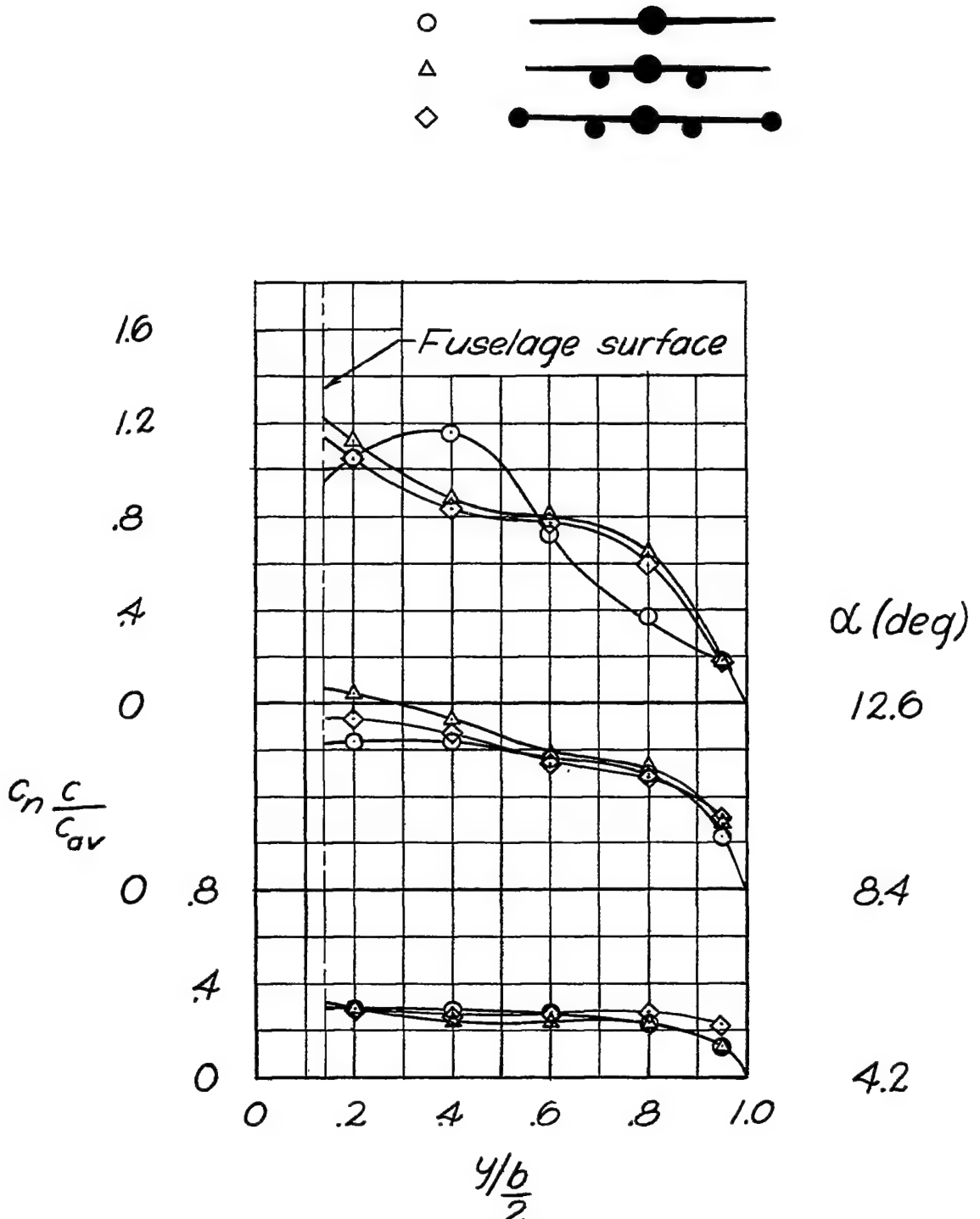


Figure 4.- Continued.

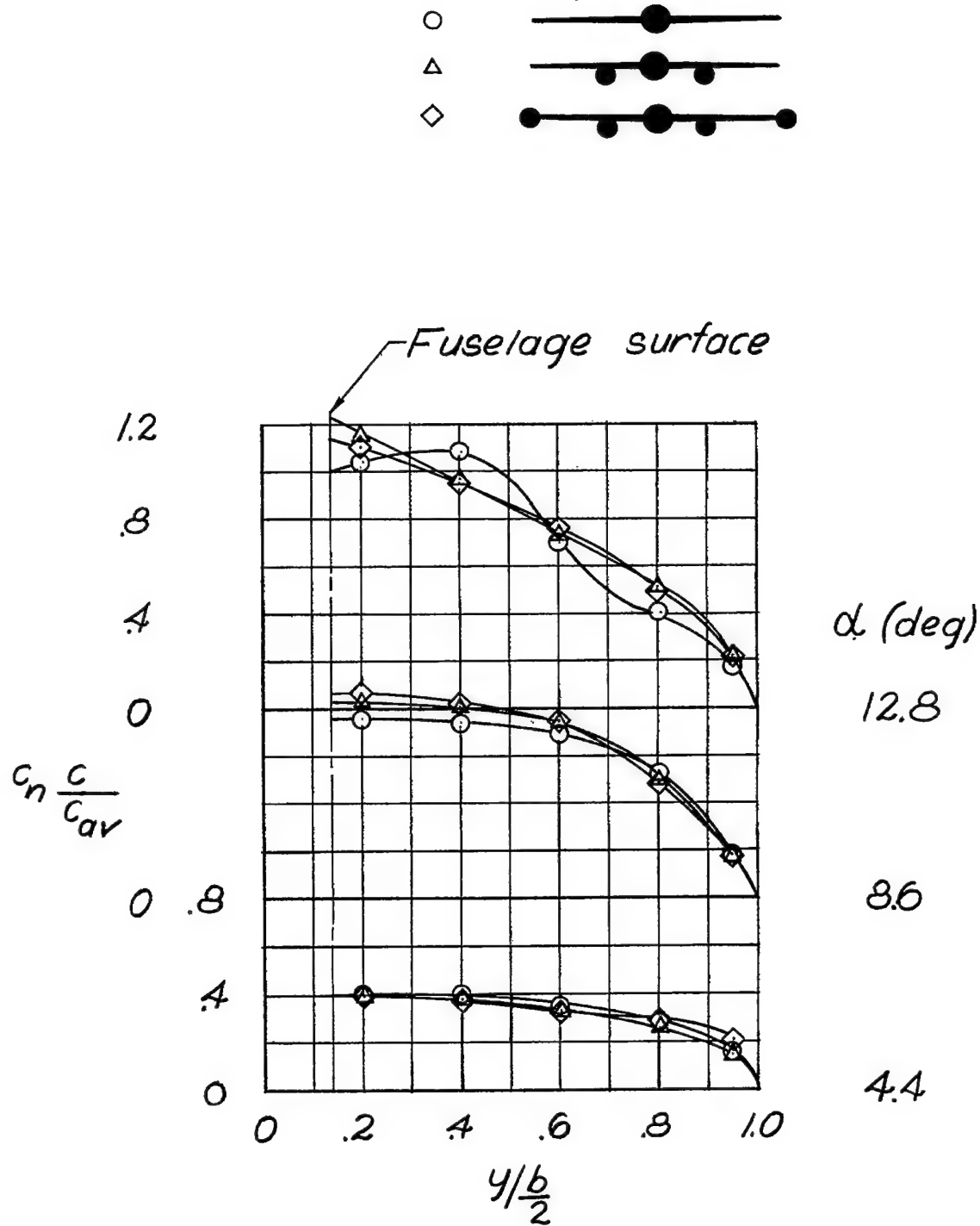
(c)  $M = 0.91.$ 

Figure 4.- Concluded.

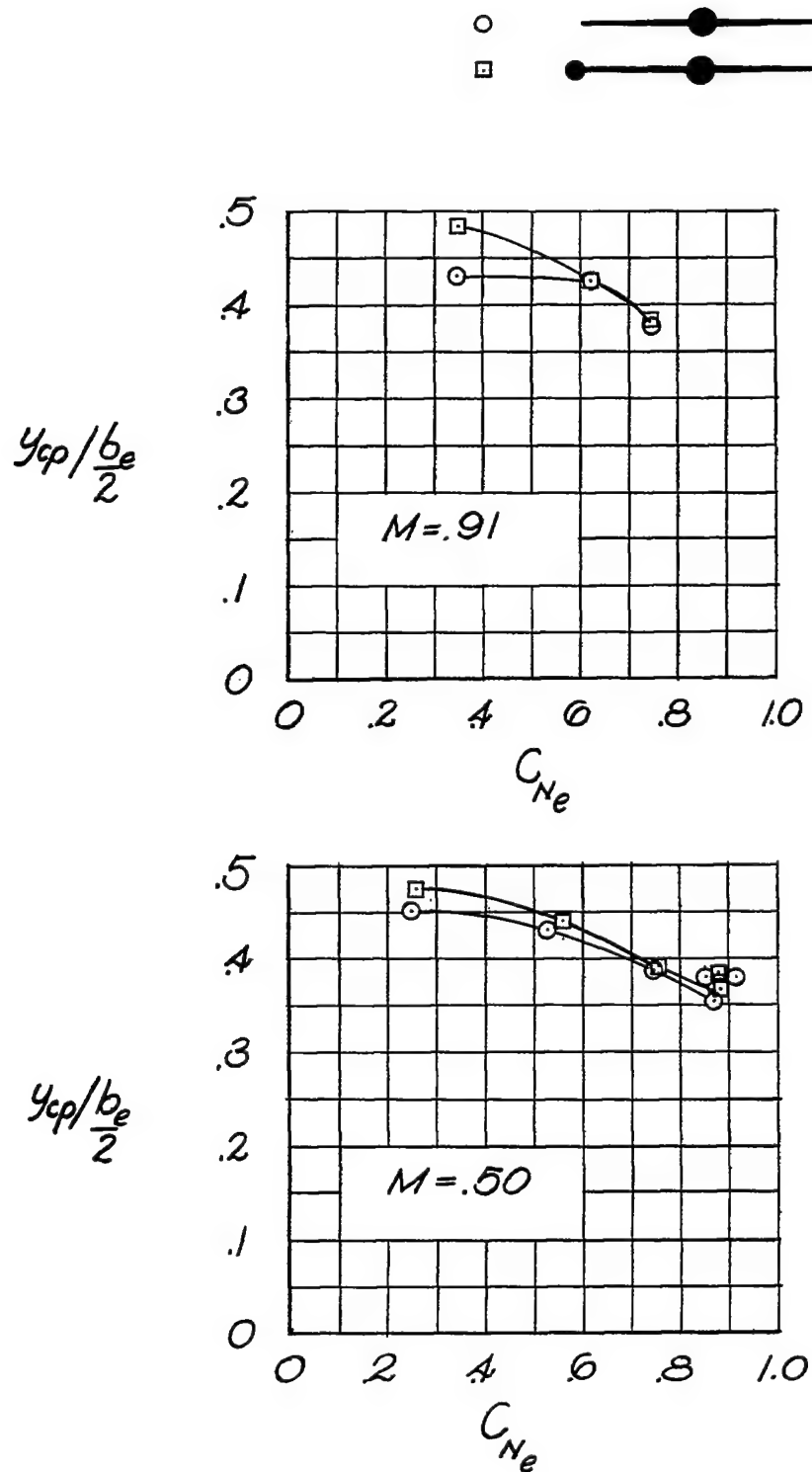


Figure 5.- Location of the lateral centers of pressure of the model without external stores and with the tip external stores.

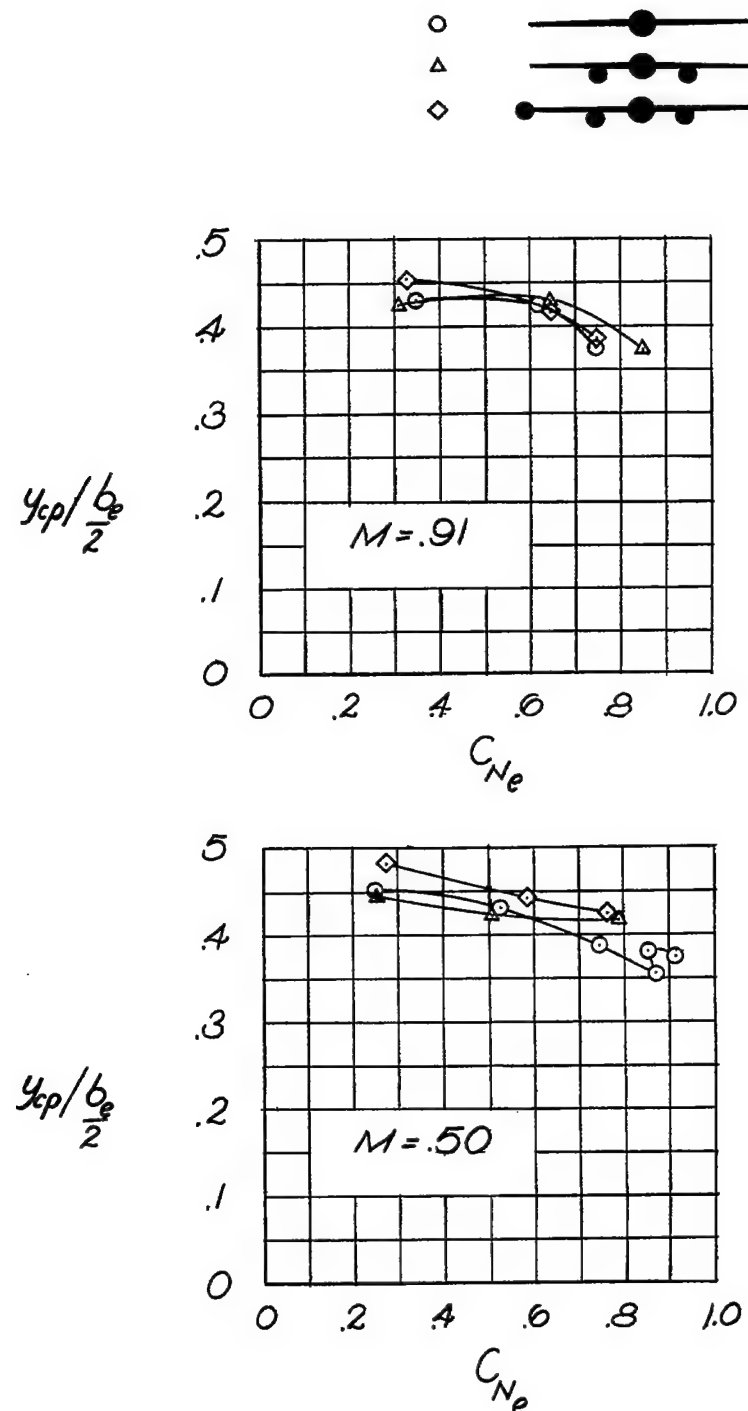


Figure 6.- Location of the lateral centers of pressure of the model without external stores, with the inboard external stores, and with the inboard and tip external stores in combination.

$$\Delta \left( \frac{C_n}{C_{Ne}} \frac{c}{C_{av}} \right) = \left( \frac{C_n}{C_{Ne}} \frac{c}{C_{av}} \right)_{model+store} - \left( \frac{C_n}{C_{Ne}} \frac{c}{C_{av}} \right)_{model}$$

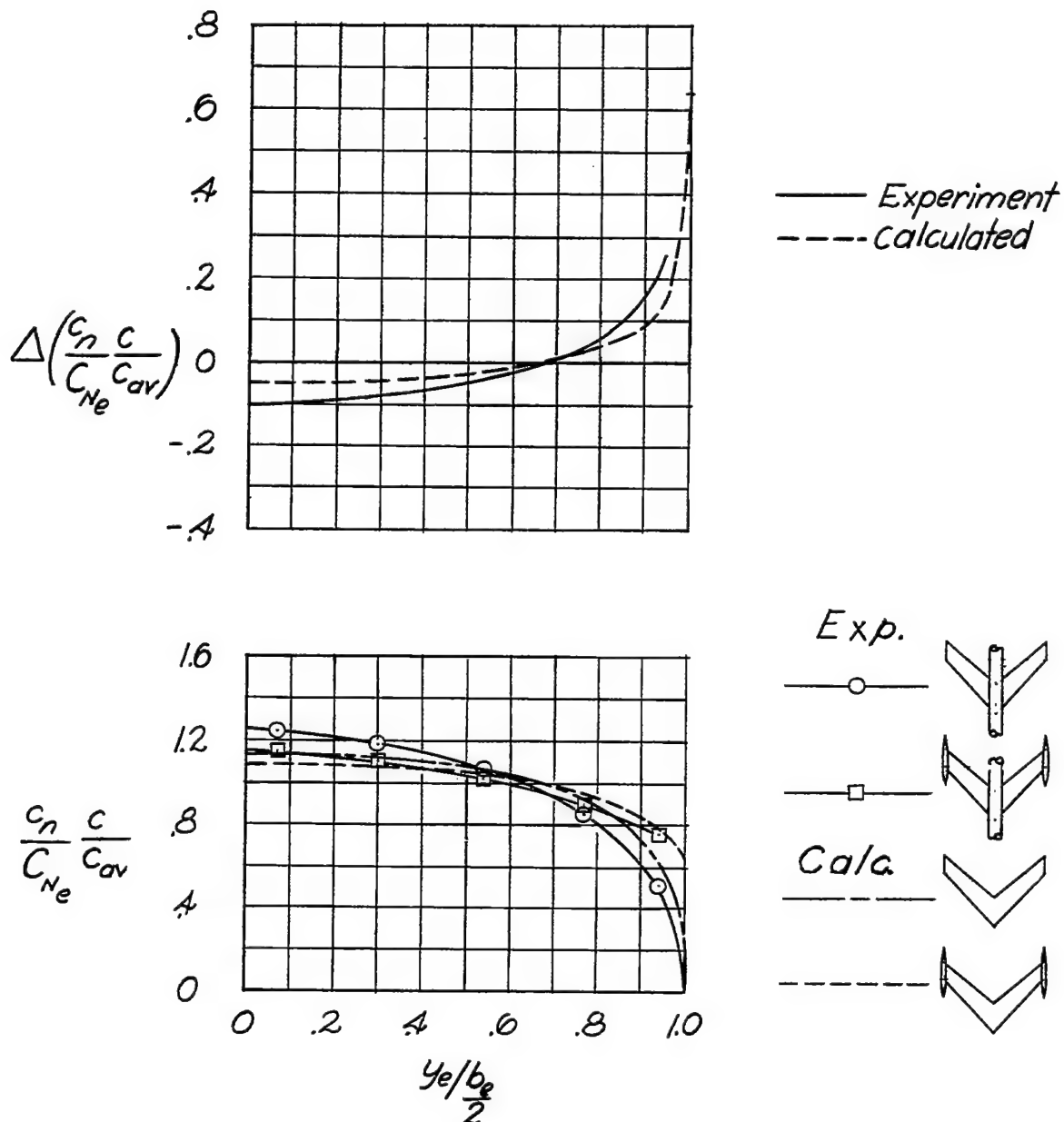


Figure 7.- Effect of tip external stores on the span loading characteristics.  
 $\alpha = 4.2^\circ$ ;  $M = 0.50$ .

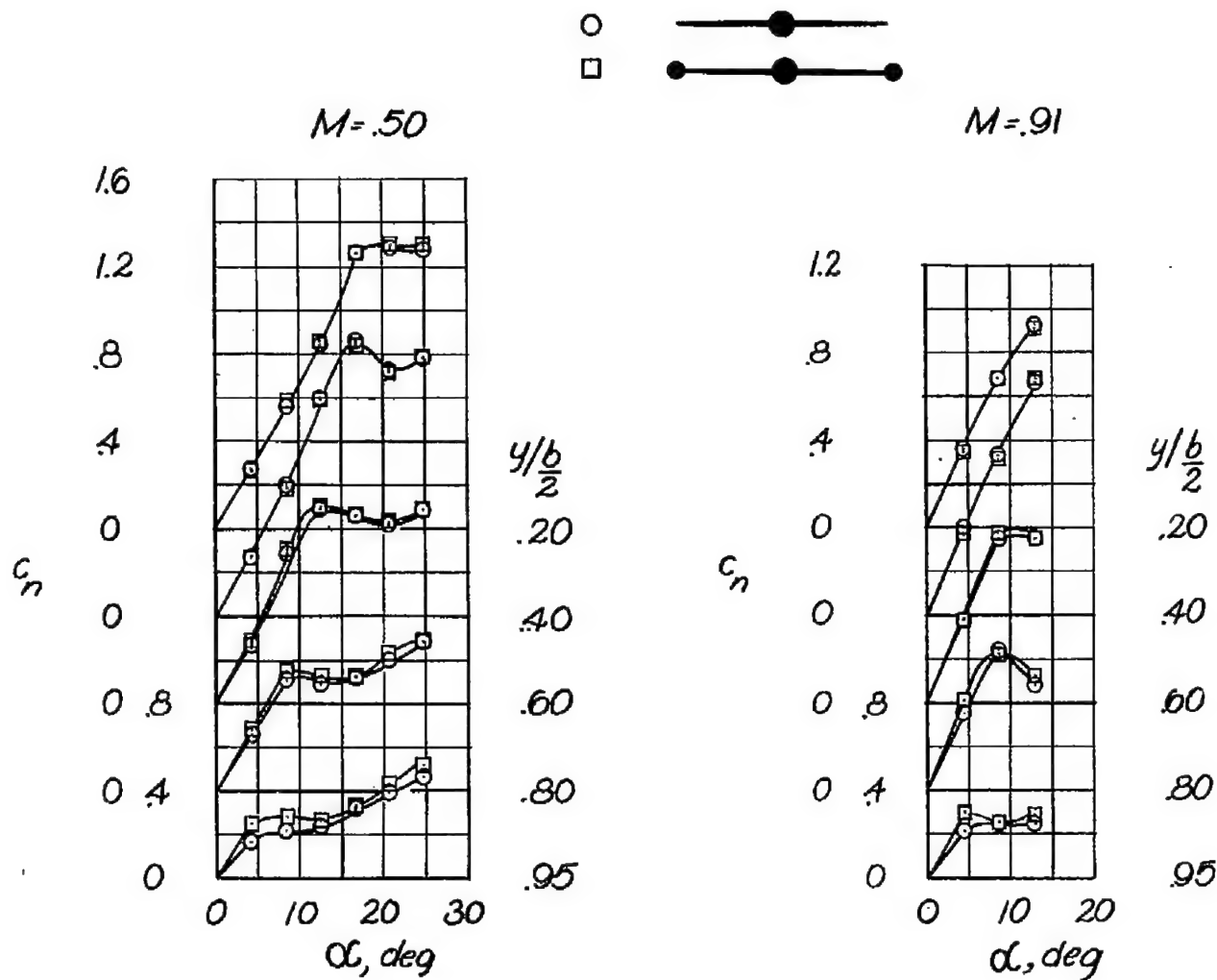


Figure 8.- Variation of the section normal-force coefficient with angle of attack for the model without external stores and with the tip external stores.

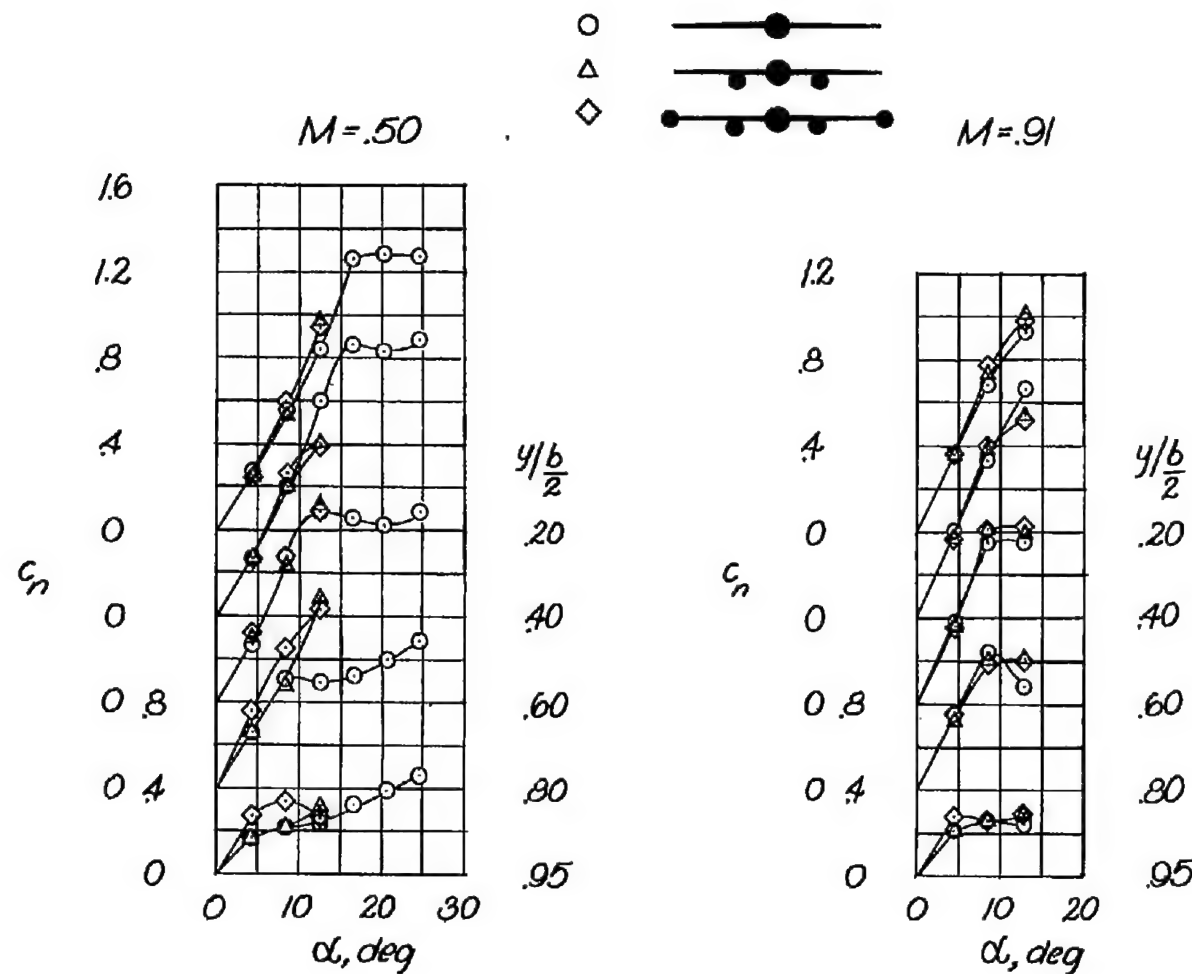


Figure 9.- Variation of the section normal-force coefficient with angle of attack for the model without external stores and with the inboard external stores, and with the inboard and tip external stores in combination.

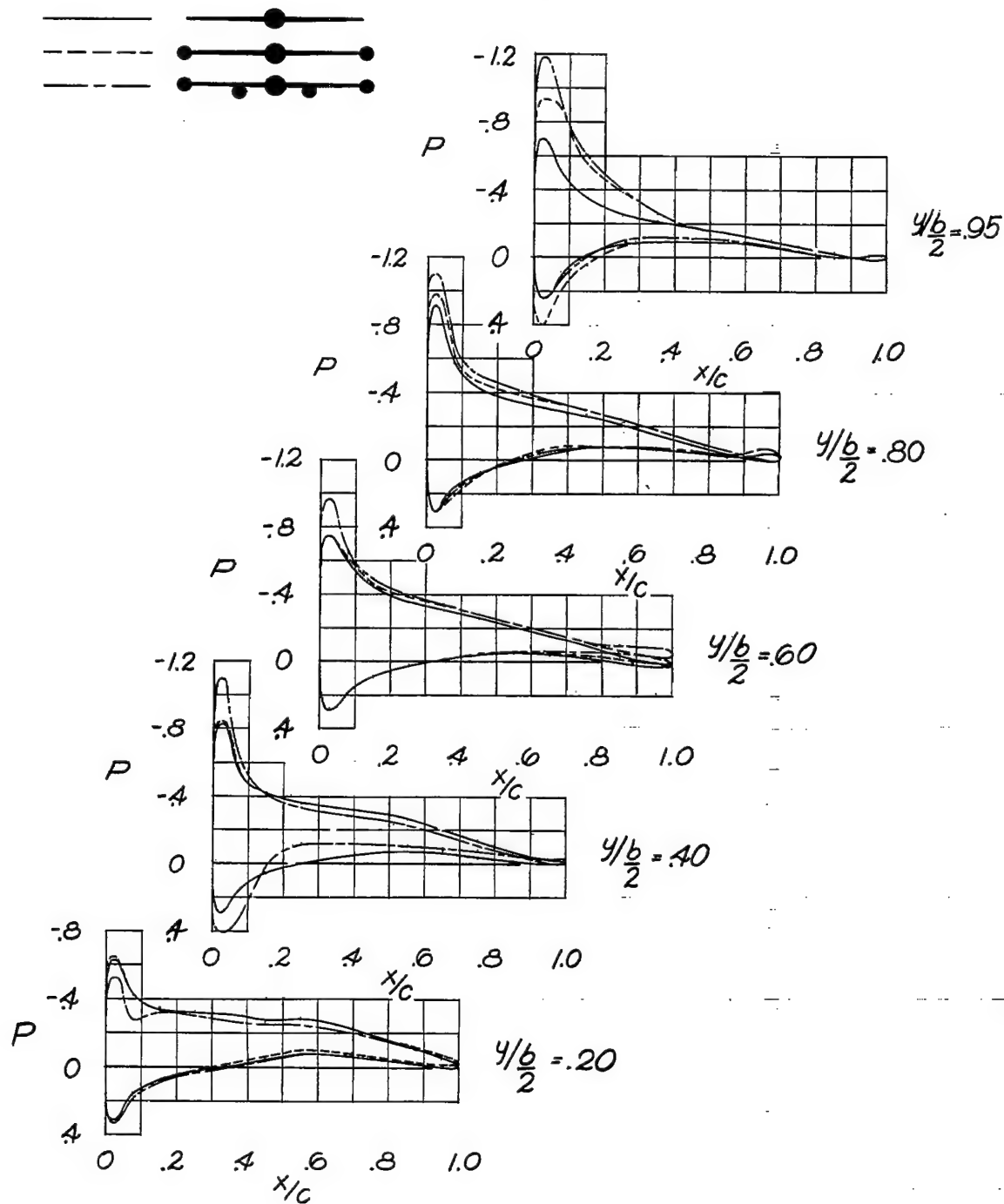
(a)  $M = 0.50$ .

Figure 10.- Chord loading at a nominal angle of attack of  $4^{\circ}$  of the model without external stores, with the tip external stores, and with the inboard and the tip external stores in combination.

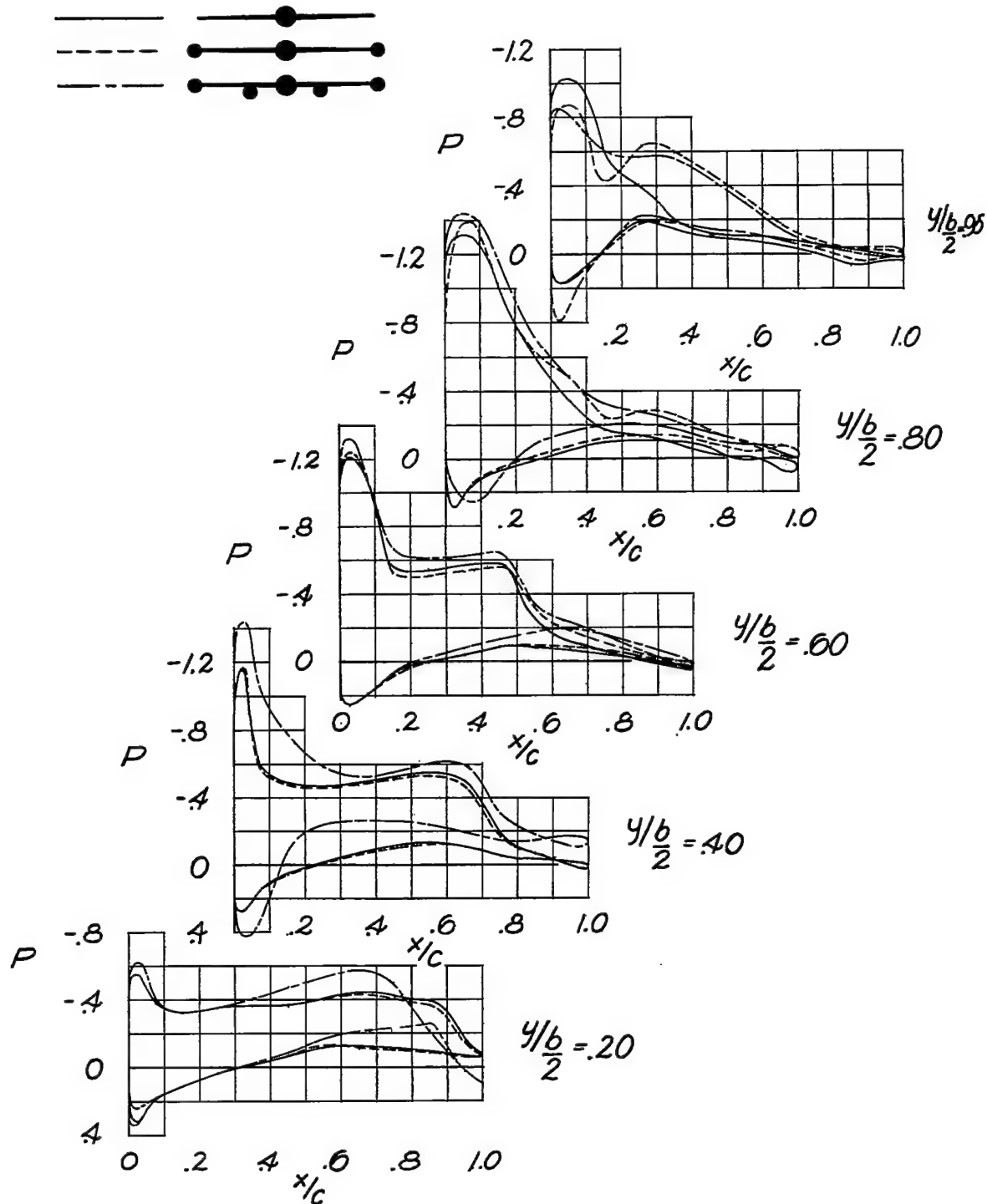
(b)  $M = 0.91$ .

Figure 10.- Concluded.

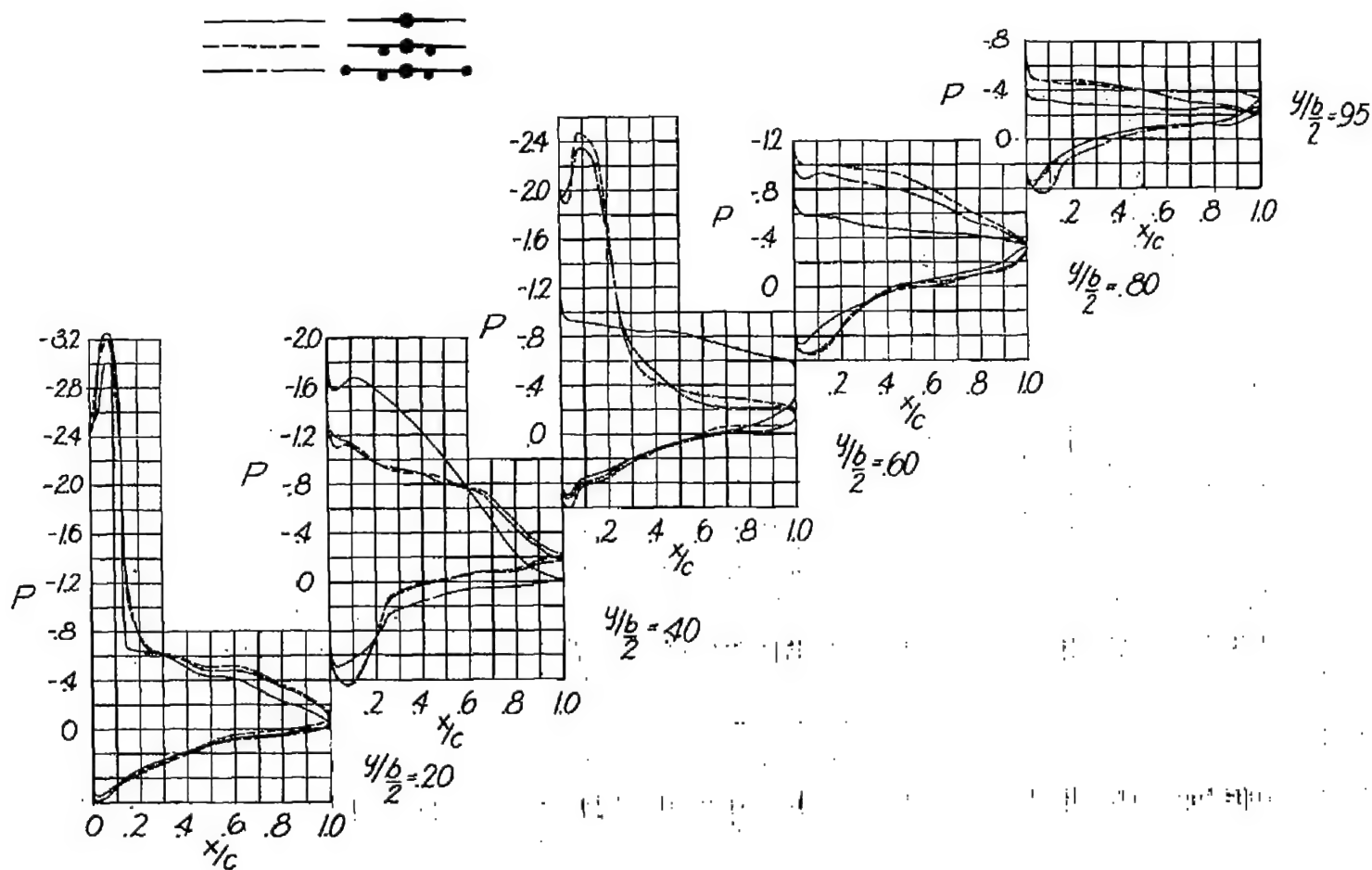
(a)  $M = 0.50$ .

Figure 11.-- Chord loading at a nominal angle of attack of  $12^{\circ}$  of the model without external stores, with the inboard external stores, and with the inboard and the tip external stores in combination.

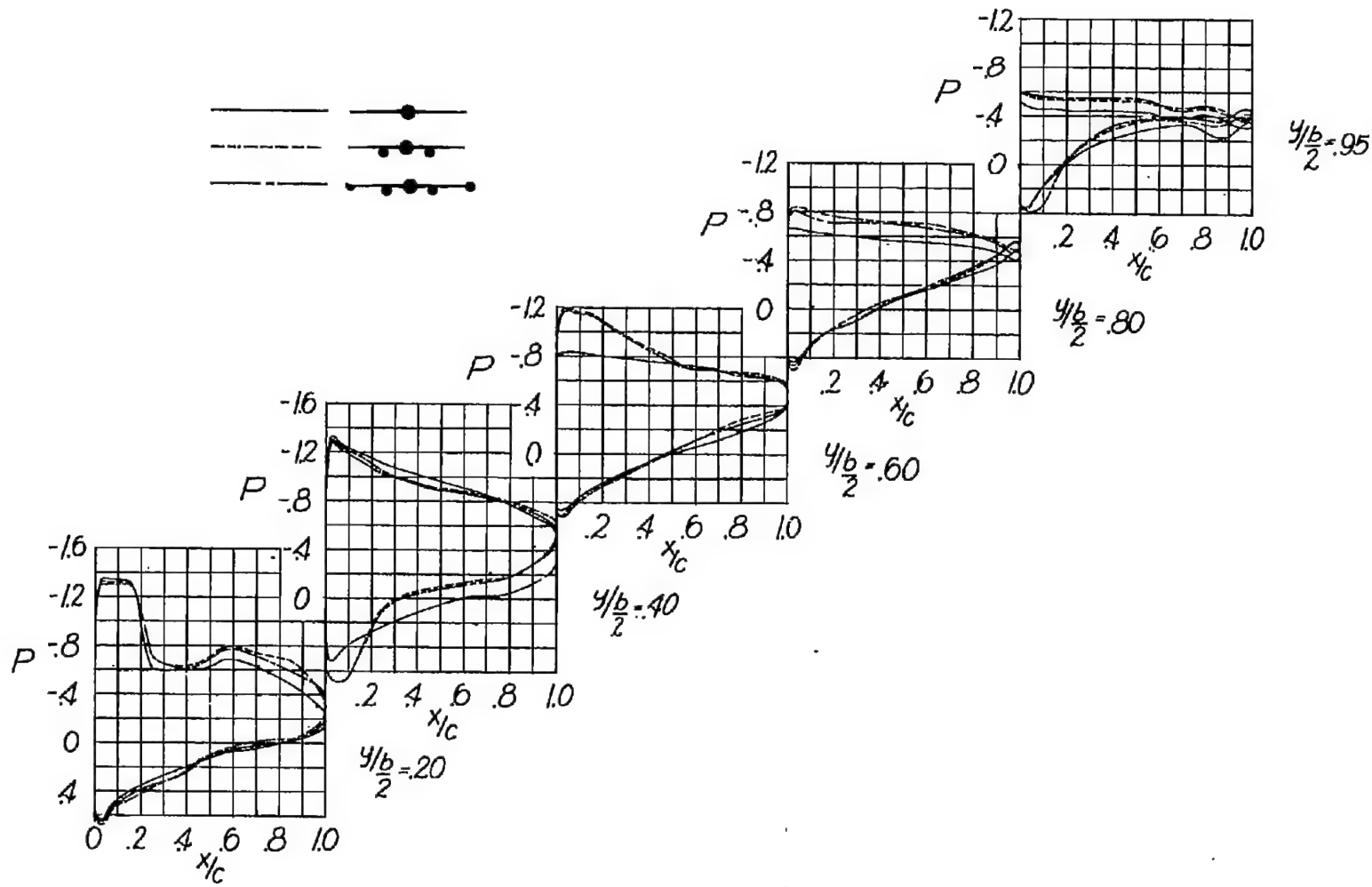
(b)  $M = 0.91$ .

Figure 11.- Concluded.

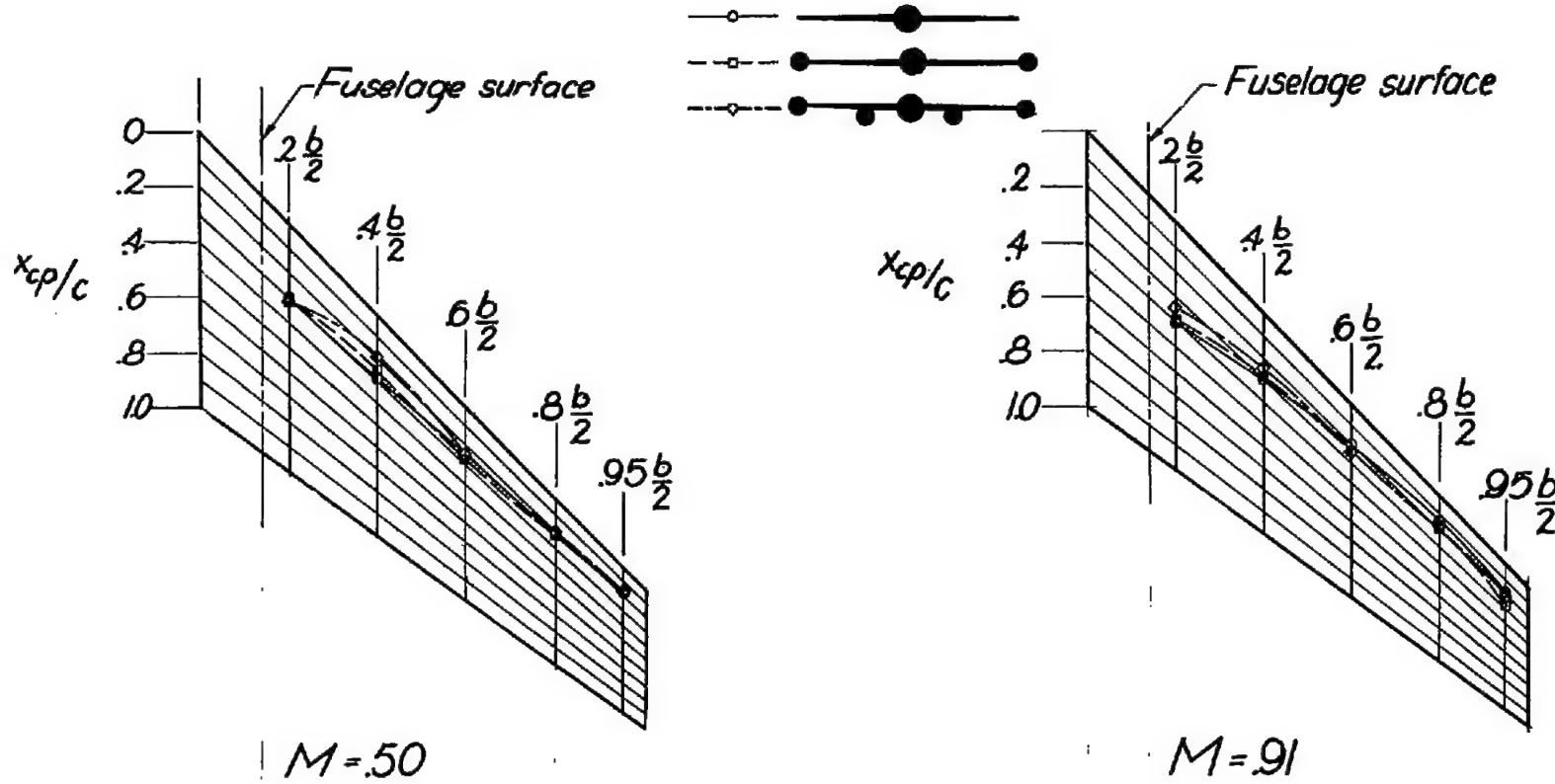


Figure 12.- Chordwise locations of the centers of pressure at a nominal angle of attack of  $4^{\circ}$  for the model without external stores, with the tip external stores, and with the inboard and the tip external stores in combination.

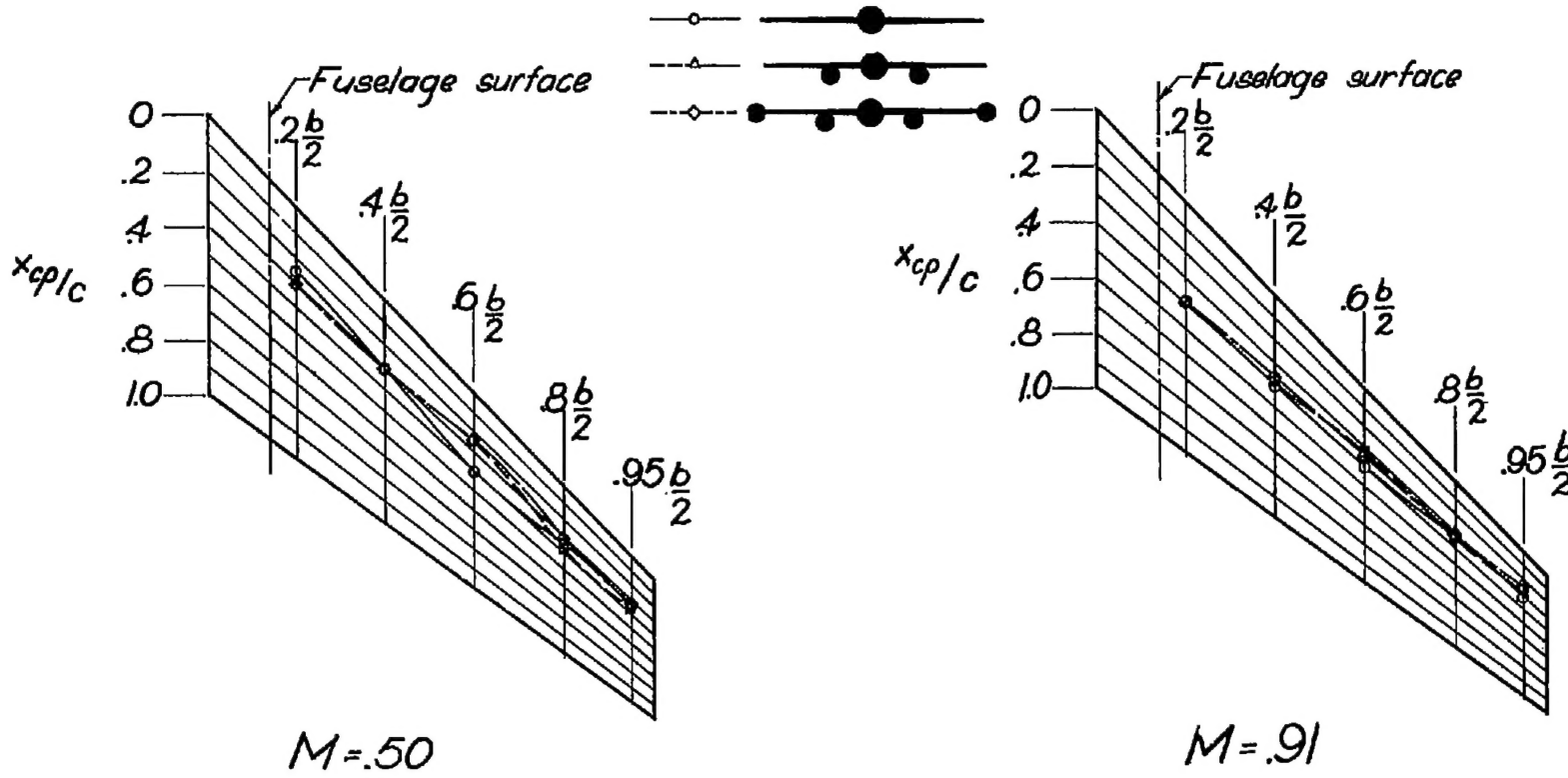


Figure 13.- Chordwise locations of the centers of pressure at a nominal angle of attack of  $12^\circ$  for the model without external stores, with the inboard external stores, and with the inboard and tip external stores in combination.

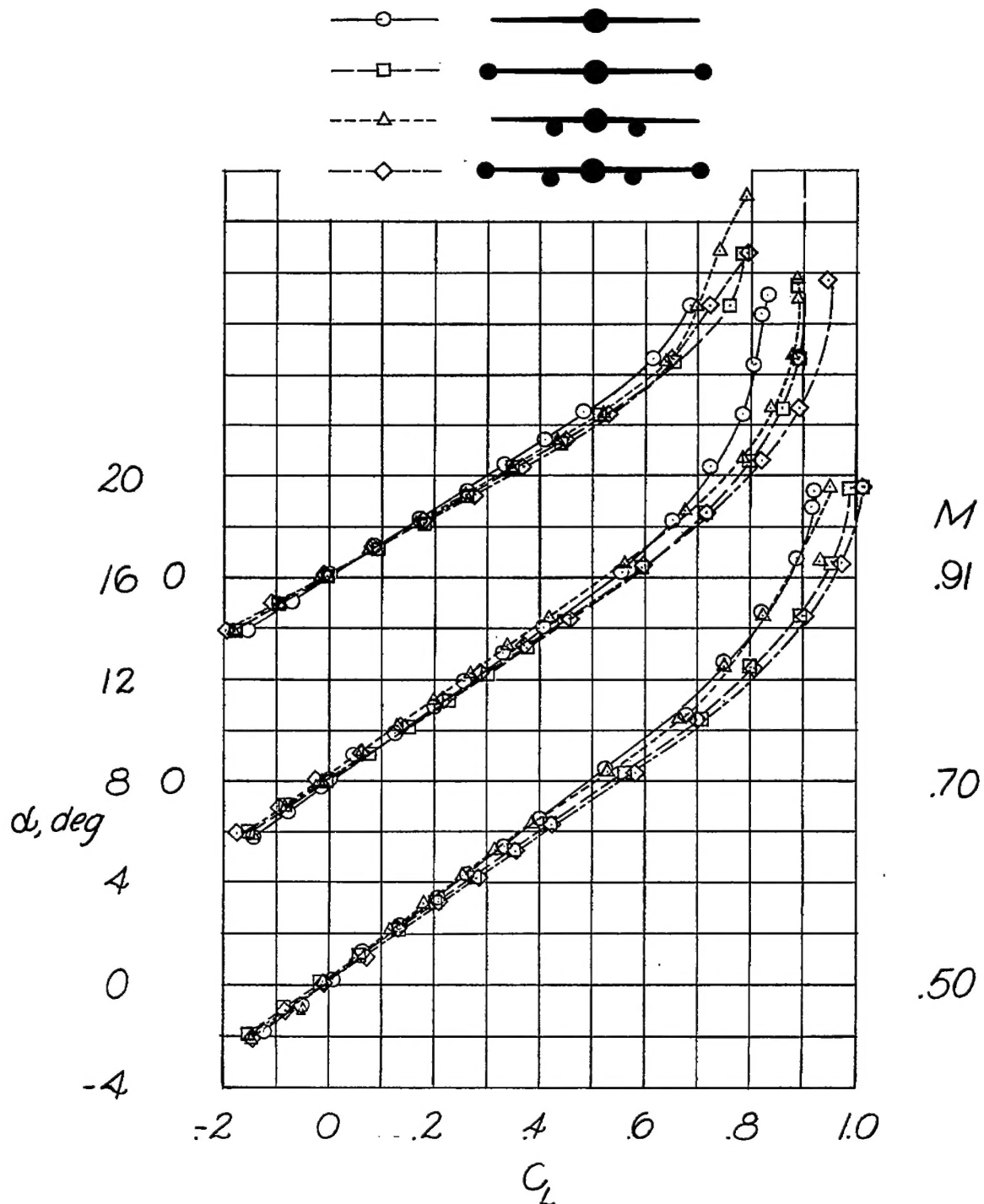
~~CONFIDENTIAL~~

Figure 14.- Aerodynamic characteristics of the model without external stores and with the various arrangements of the external stores.

~~CONFIDENTIAL~~

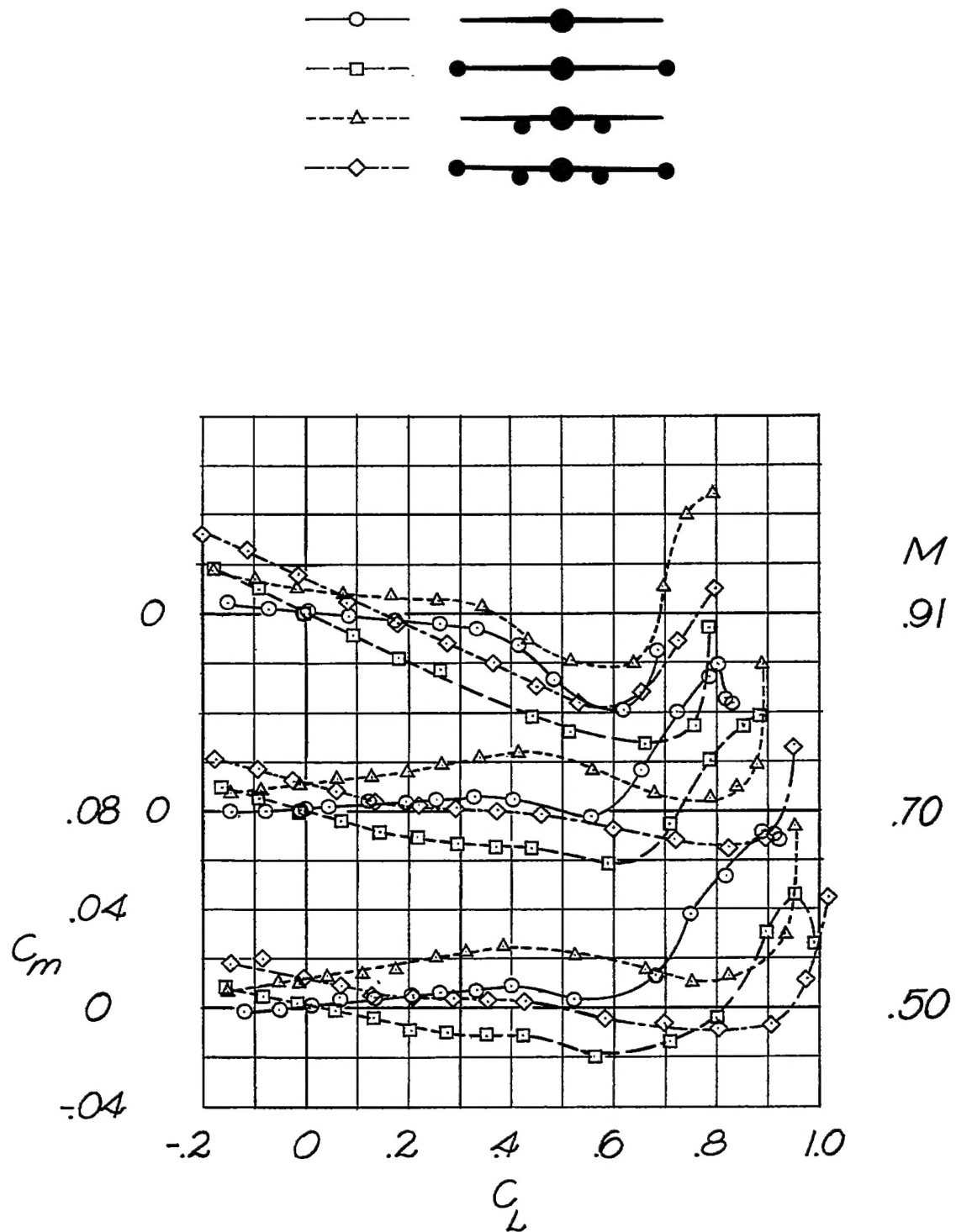


Figure 14.- Concluded.

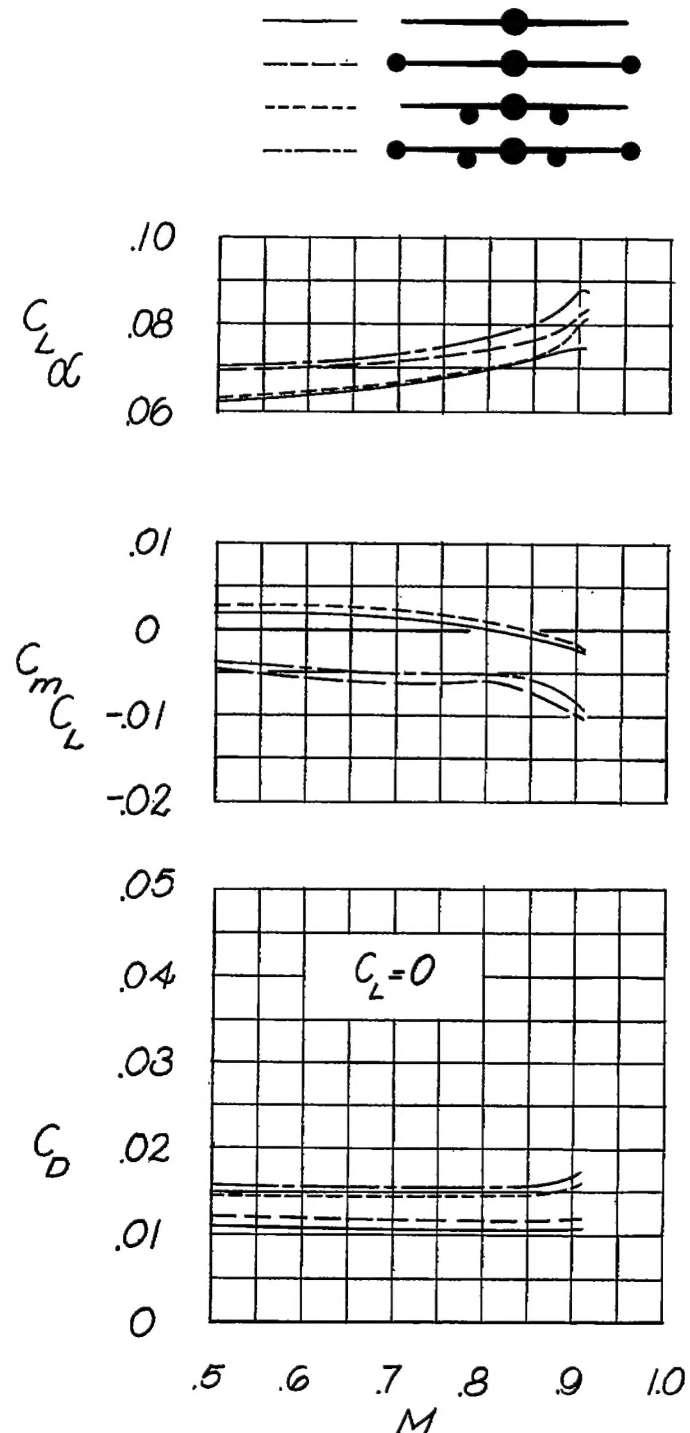


Figure 15.- Summary of the aerodynamic characteristics of the models without external stores and with the various arrangements of the external stores.